Clayfield, E. J., and E. C. Lumb, "Detachment of Adhered Colloidal Particles by Non-acqueous Surfactant Solutions," *Disc. Faraday Soc.*, **42**, 285 (1966).
DiMarzio, E. A., and C. M. Guttman, "Separation by Flow," *Macromolecules*, **3**, 131, 681 (1970).
Friis, N., and A. E. Hamielic, "Gel Permeation Chromatography-A Review of Axial Dispersion Phenomena, Its Detection and Correction," *Adv. Chromatography*, **13**, 41 (1975).
Fowkes, F. M., "Attractive Forces at Interfaces," *Ind. Eng. Chem.*, **56**, No. 12, 40 (1964).
Gee, D., "Adsorption in the Secondary Minima of Polystyrene Lattices on Polystyrene Divinylbenzene Copolymer Packing Beads," Rept. on NSF Undergraduate Summer Research, Emulsion Polymers Institute, Lehigh University, Bethlehem, Pa. (1976).
Goldman, A. J., R. G. Cox, and H. Brenner, "Slow Viscous Motion of a Sphere Parallel to a Plane Wall, II, Couette Flow," *Chem. Eng. Sci.*, **22**, 653 (1967).
Goldsmith, H. L., and S. G. Mason, "The Flow of Suspensions Through Tubes, I, Single Spheres, Rods, and Discs," *J. Colloid Interface Sci.*, **17**, 448 (1962).
Hamaker, H. C., "The London-van der Waal's Attraction between Spherical Particles," *Physica*, **4**, 1058 (1937).
Krebs, V. K. F., and W. Wunderlich, "Die Ermittlung der Teilchengroßenverteilung von Polymer-Dispersionen durch Gelchromatographie," *Angew. Makromol. Chem.*, **20**, 203 (1971).
Loeb, A. L., P. H. Wiersema, and J. Th. G. Overbeck, *The Electrical Double Layer around a Spherical Particle*, Mass. Inst. Technol. Press, Cambridge (1961).
McHugh, A. J., C. Silebi, G. W. Poehlein, and J. W. Vanderhoff, "Hydrodynamic Chromatography of Latex Particles," *Colloid Interface Sci.*, **IV**, 549 (1976).
———, "Hydrodynamic Chromatography (HDC) of Latex Particles," Paper presented at A.I.Ch.E. Meeting, Houston, Tex. (Mar., 1977).
Moore, J. C., "Gel Permeation Chromatography, I. A New Method for Molecular Weight Distribution of High Polymers," *J. Polymer Sci.*, **A2**, 835 (1964).
Ottewill, R. H., and J. N. Shaw, "Stability of Monodisperse Polystyrene Latex Dispersions of Various Sizes," *Disc. Faraday Soc.*, **42**, 154 (1966).
Prieve, D. C., and E. Ruckenstein, "Role of Physical Interactions in Reversible Adsorption of Hydrosals or Globular Proteins: Application to Chromatographic Separations," *Colloid Interface Sci.*, **IV** (1976).
Ruckenstein, E., and D. C. Prieve, "Adsorption and Desorption of Particles and Their Chromatographic Separation," *AIChE J.*, **22**, 276 (1976).
Schaller, E. J., and A. E. Humprey, "Electroviscous Effects in Suspension of Monodisperse Spherical Particles," *J. Colloid Interface Sci.*, **22**, 573 (1966).
Schenkel, J. H., and J. A. Kitchener, "A Test of the Derjaguin-Verwey-Overbeck Theory with a Colloidal Suspension," *Trans. Faraday Soc.*, **56**, 161 (1960).
Scolere, J., "Hydrodynamic Chromatography" M.S. thesis Lehigh Univ., Bethlehem, Pa. (1977).
Silebi, C. A., Mathematical Modeling of Hydrodynamic Chromatography," Ph.D. thesis in preparation, Lehigh Univ., Bethlehem, Pa. (1977).
———, and A. J. McHugh, "The Analysis of Particle Size Distributions in Hydrodynamic Chromatography," submitted to *J. Appl. Polym. Sci.*
Small, H., "Hydrodynamic Chromatography, a Technique for Size Analysis of Colloidal Particles," *J. Colloid Interface Sci.*, **48**, 147 (1974).
Stoisits, R. F., G. W. Poehlein, and J. W. Vanderhoff, "Mathematical Modeling of Hydrodynamic Chromatography," *J. Colloid Interface Sci.*, **57**, 337 (1976).
Verwey, E. J. W., and J. Th. G. Overbeck, *Theory of the Stability of Lyophobic Colloids*, Elsevier, Amsterdam (1948).
Visser, J., "On Hamaker Constants: A Comparison between Hamaker Constants and Lifshitz-van der Waal's Constants," *Adv. Colloid Interface Sci.*, **3**, 331 (1972).
Wiese, G. R., and T. W. Healy, "Effect of Particle Size on Colloid Stability," *Trans. Faraday Soc.*, **66**, 490 (1970).

Manuscript received May 25, 1977; revision received and accepted November 14, 1977.

Kinetic, Transport, and Deactivation Rate Interactions on Steady State and Transient Responses in Heterogeneous Catalysis

J. W. LEE
J. B. BUTT
and
D. M. DOWNING

Department of Chemical Engineering and Ipatieff Catalytic Laboratory Northwestern University Evanston, Illinois 60201

SCOPE

The classical theory of diffusion and heterogeneous catalytic reaction has been primarily concerned with the interaction between chemical and physical rate processes in a time invariant system. In practice, however, various mechanisms act to alter activity and selectivity patterns, and one should append to the analysis yet another rate process, that of deactivation.

The present research is an experimental and modeling study of the effects of impurity poisoning on the steady state and transient behavior of a diffusionally influenced, exothermic, catalytic reaction. Major factors included in

Correspondence concerning this paper should be addressed to J. B. Butt. J. W. Lee is with Mobil Research and Development Corp., Paulsboro, New Jersey 08065. D. M. Downing is with Exxon Research and Engineering Co., Baton Rouge, Louisiana 70821.

0001-1541-78-1009-0212-$01.35

the study are how transient response time scales and magnitudes are affected by differing levels of deactivation, what is the alteration in the magnitude of intra and interphase gradients on progressive deactivation, and what level of effort is required in simulation to present differing levels of detail on the effects of poisoning on catalyst behavior.

Benzene hydrogenation over a nickel/kieselguhr catalyst, poisoned by thiophene, used in these experiments is representative of the class of exothermic catalytic reactions subject to irreversible poisoning. By changing the concentration of poison in the reaction mixture, it is possible to change the time scale of the deactivation; in the present work, this parameter was fixed so as to permit a quasistationary state assumption for the kinetics of deactivation.

CONCLUSIONS AND SIGNIFICANCE

Steady state and transient response behavior in catalysis are strongly influenced by catalyst deactivation. In the present experiments, the time required for development of steady state profiles on start-up decreased only moderately as the catalyst was poisoned to about 20% of initial activity. The magnitudes of inter and intraphase thermal gradients, however, were strongly affected; a rather surprising result is that the ratio of intra to interphase ΔT increases with deactivation. This is due at least partially to the very nonuniform (spatial) distribution of activity within the poisoned particle. For severely deactivated catalysts, the approximation that all thermal gradients reside in the boundary layer is not justified.

Simulation results from a full distributed parameter model are excellent for the steady state modeling and for transient responses of the fresh catalyst; however, they deteriorate somewhat for experiments with highly deactivated catalysts. Even though poisoning is rapid and irreversible under the conditions employed here, a shell-progressive model may not be adequate if one wishes to simulate in full detail activity and thermal gradients in both steady and unsteady states. On the other hand, such an approach appears entirely adequate if only information on the overall time-activity history is required.

The summation of present knowledge concerning the theory (and a good deal of the experiment) of diffusion and reaction in heterogeneous catalysis has recently been presented by Aris (1975). From that elegant work it is clear that further experimental information with interpretation, particularly concerning unsteady state behavior, is a major need. The present work is directed toward elucidation of the simultaneous interaction between four rate processes associated with heterogeneous catalysis: the rate of the catalytic reaction, the rates of inter-intraphase heat and mass transport, and the rate of catalyst deactivation. Both steady state and transient responses will be examined in experiment and in simulation.

The experiments performed rest upon the measurement of intraparticle temperature profiles and interphase temperature gradients in a single-pellet reactor following the methods previously described by Irving and Butt (1967) and Kehoe and Butt (1972). As in prior work, the hydrogenation of benzene on a nickel/kieselguhr catalyst was used as a representative model exothermic reaction system; thiophene was used as a poison for the catalyst in the experiments described here. A number of other reactions have been investigated via intraparticle temperature measurements in recent years, including ethylene hydrogenation on nickel/silica-alumina (Hughes and Koh, 1970, 1974), carbon monoxide oxidation on copper oxide-alumina (Benham and Denny, 1972), and oxidative dehydrogenation of butene to butadiene on tin antimony oxide (Trimm et al., 1974). Steady state temperature profiles in the nickel/silica-alumina catalyst poisoned by oxygen were reported by Koh and Hughes (1974); the intraparticle temperature rises of both fresh and deactivated catalysts were not much different from each other.

Prior studies of intraparticle deactivation problems were summarized by Butt in 1972. Since that time, Petersen and co-workers (1973, 1974) have studied the deactivation of platinum/η-alumina catalysts by coking in the hydrogenation of cyclopropane. Their results, in comparison with the present data on poisoning, point to the very substantial differences in the influence of the mechanism of deactivation on catalytic performance.

EXPERIMENTAL

The single-pellet reactor system, method of pellet instrumentation and of temperature measurement, reagents and their

Table 1. Summary of Experimental Conditions Investigated

Run	T_F, °C	Activity (s)	$(x_B)_F$	$(x_T)_F$	Time on stream, min
General range (all runs)	50-188	1.0-0.10	0.05-0.25	0.01	0-420
Runs illustrated					
1SC	85	1.0	0.16	—	—
1SI	50	1.0	0.16	—	—
2-DEF2	188	1.0	0.08	—	—
2U	110	1.0	0.12	—	—
2P	110	0.10	0.16	0.01	420
6-DEF4	100	1.0	0.16	—	—
6P1	100	0.40	0.16	0.01	18
6P4	85	0.40	0.16	0.01	18
6P5	75	0.40	0.24	0.01	18
6U1	65	1.0	0.16	—	—
6U2	65	0.40	0.16	0.01	18
6U3	65	0.16	0.16	0.01	90
6PP3	100	0.16	0.16	0.01	90
6PP5	100	0.16	0.16	0 01	90
6PP6	85	0.16	0.16	0.01	90

Notes: Experiments were run at both 3 and 6 l/min flow rate (inlet) to reactor. Well-mixed conditions existed in the bulk gas phase within the reactor under both flow rates. 6U2 and 6U3 represent activities of 0.40 and 0.16 in run 6U; no transient response experiments were run at these conditions.

TABLE 2. CATALYST PARAMETERS

Physical form: 1.27 cm diam by 6 to 6.5 cm cylinders, prepared from Harshaw Ni-0104 P Ni/kieselguhr, 58% (wt) Ni, 24 m^2 Ni/g (reduced)

Density: $1.71 \pm 0.03 \times 10^{-3}$ kg/m^3

Heat capacity: 0.604×10^3 J/kg-°C

Effective diffusivity: $3\text{-}4 \times 10^{-6}$ m^2/s

Effective thermal conductivity: $17.6 \pm 0.8 \times 10^{-2}$ J/m-s-°C

Micropore characteristics
- Porosity: 0.22
- Average pore radius: 6 nm

Macropore characteristics
- Porosity: 0.34
- Average pore radius: 315 nm

Notes: Effective diffusivity determined from random pore model (Lee, 1976). Effective thermal conductivity measured using thermal comparator by Dr. Y. S. Touloukian, Properties Research Laboratory, Purdue University. Porosity and pore size distribution measured by mercury porosimity and nitrogen desorption by Dr. D. K. Kim, Research Department, Amoco Oil Company. Heat capacities calculated from tabulated specific heat data for individual components (Lee, 1976).

quality, and general experimental procedures were similar to those described by Kehoe and Butt (1972*a*) and are discussed in detail by Lee (1976). The major modification was provision of a dual feed system to the reactor so that feed could be switched from a thiophene free mixture of benzene and hydrogen to one containing the poison on an intermittent basis.

Several different types of experiments were run. Steady state temperature profiles for fresh and deactivated catalysts were determined in all experiments (representing the final state of transient measurements); start-up experiments measured the development of temperature profiles in both fresh and

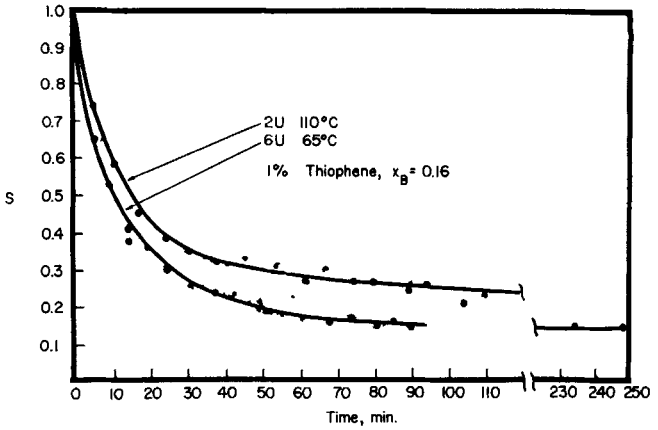

Fig. 1. Variation of the overall activity with time on stream: $(x_B)_F = 0.16$, $(x_T)_F = 0.01$.

deactivated catalysts on introduction of benzene to a catalyst initially in flowing hydrogen; perturbation experiments measured the response of temperature profiles to step changes in concentration and/or flow rate starting at a given initial steady state. On deactivated catalysts, these measurements were made with a poison free feed after the catalyst had been predeactivated to a specified level. In all experiments, temperature at six positions within the particle, in the bulk gas phase within the reactor, and at the reactor entrance, and inlet and exit compositions (allowing determination of the global rate of reaction) were measured. In addition, the internal sulfur profiles were determined for a number of deactivated particles via scanning electron microscopy. In all, some sixty different sets of conditions, corresponding to the general ranges shown in Table 1, were investigated for fresh and deactivated catalysts via the combination of steady state, start-up, and perturbation experiments. Catalyst parameters are given in Table 2. The results of experiment and simulation presented here are chosen to be representative of the overall program described by Lee (1976).

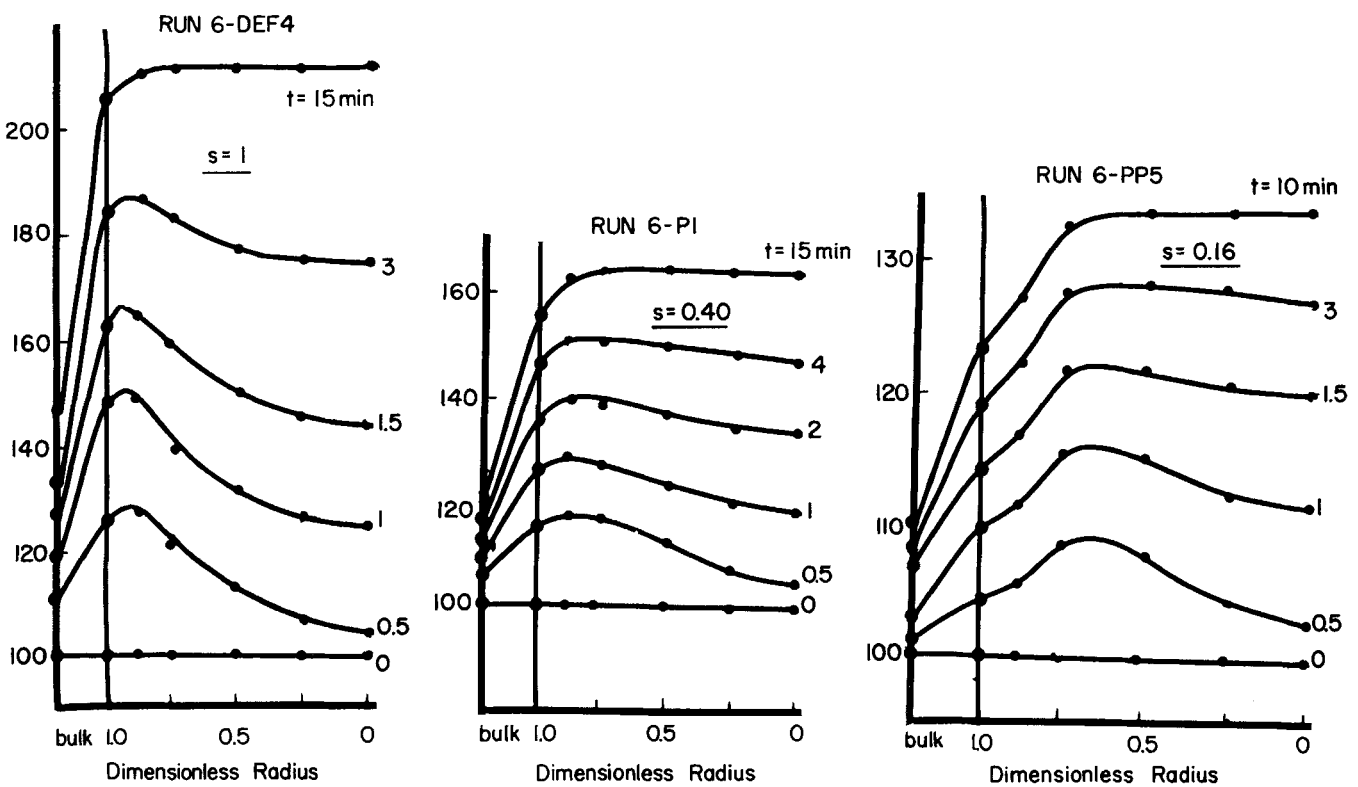

Fig. 2. Effect of deactivation on start-up transients: $T_F = 100$°C, $(x_B)_F = 0.16$, $(x_T)_F = 0.01$.

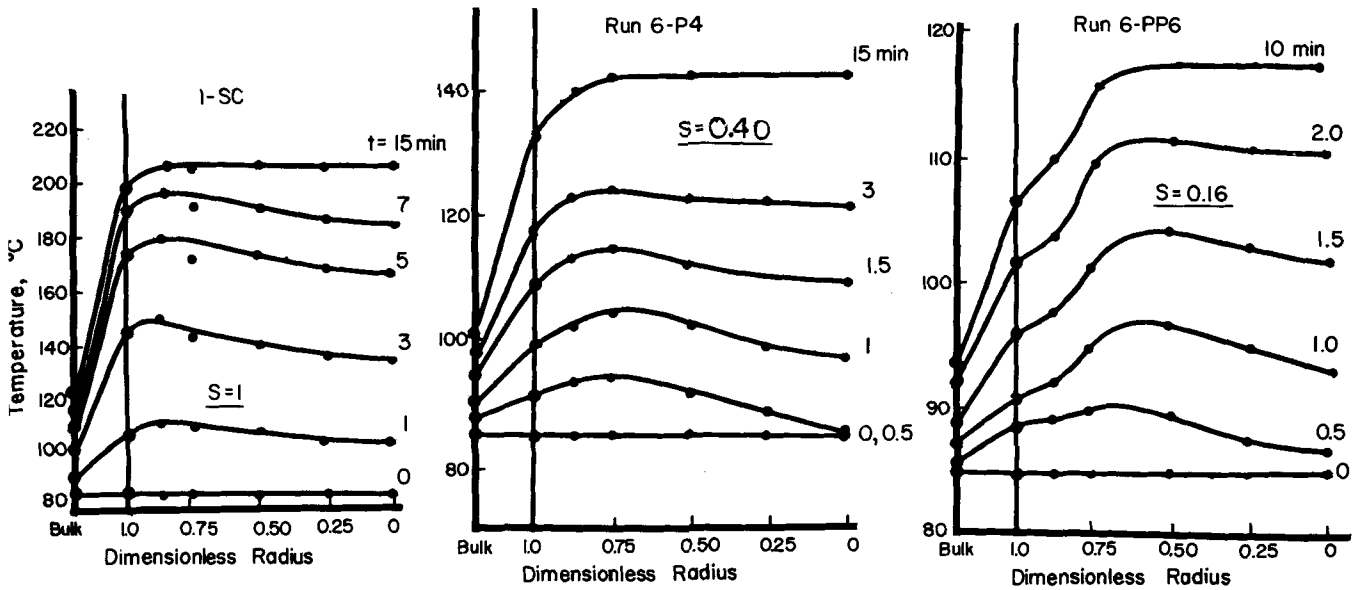

Fig. 3. Effect of deactivation on start-up transients: $T_F = 85°C$, $(x_B)_F = 0.16$, $(x_T)_F = 0.01$.

RESULTS

Overall Activity Variation

The general characteristics of activity variation on thiophene poisoning for two series of experiments with identical feed compositions but differing reactor inlet temperatures are shown in Figure 1. There is an initial very rapid loss of activity in each case, which is seen to stabilize after about a ½ hr of operation. The activity variable s shown in the figure is just the overall rate of reaction at time t divided by the rate obtained for the fresh catalyst. This type of temporal behavior appears quite common for catalytic systems such as this in which there is a strong, near irreversible affinity between poison and catalyst (Lyubarskii, et al., 1962) and in the present instance is indicative of a shell-progressive penetration of poison into the pellet, as will be demonstrated later. The lower rate of deactivation at the higher temperature reflects lower equilibrium surface coverage at that condition and is in qualitative agreement with the results of Lyubarskii et al. (1962).

Transient Response Behavior

The nature of the transient response on start-up is shown in Figures 2 and 3 for catalysts under two sets of conditions, again differing only in feed temperature, and at three levels of activity: $s = 1.0$, 0.40, and 0.16. These are average levels of activity and do not imply, with the exception of the fresh catalyst, uniformity of activity profiles within the pellet. Indeed, the nonuniformity of activity is clearly demonstrated by the temperature response in the two experiments with $s = 0.16$,

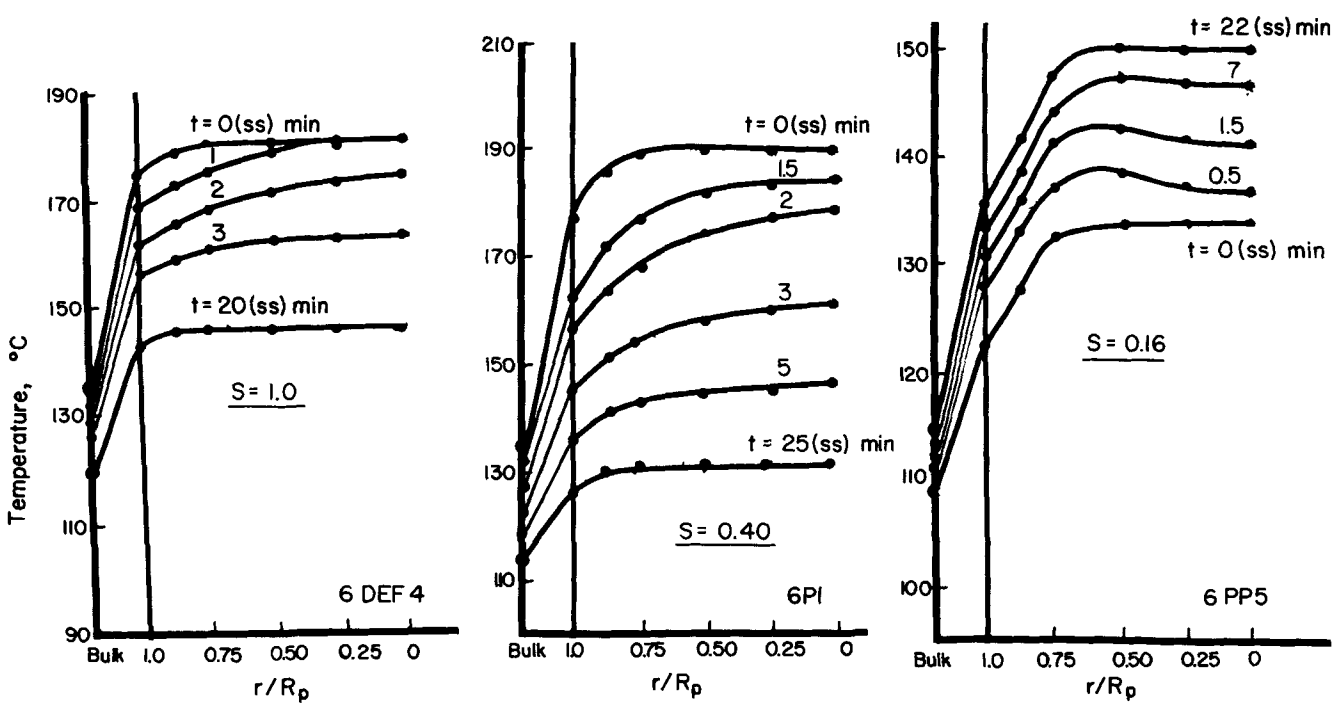

Fig. 4. Effect of deactivation on response to inlet feed concentration perturbations: $T_F = 100°C$, 6 DEF4: $(x_B)_F = 0.08 \rightarrow 0.055$, 6 P1: $(x_B)_F = 0.07 \rightarrow 0.025$, 6 PP5: $(x_B)_F = 0.16 \rightarrow 0.27$.

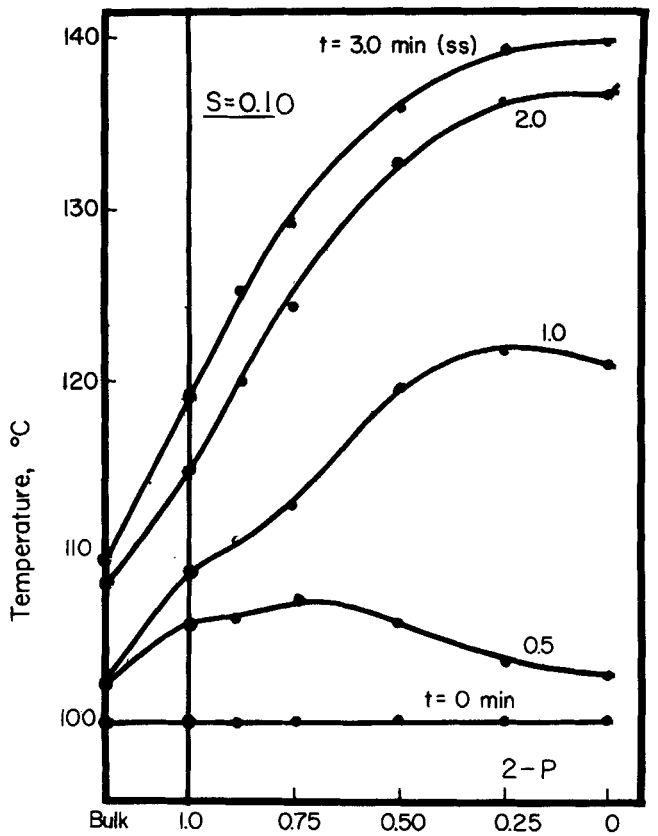

Fig. 5. An extreme example of the alteration of intraphase gradients by deactivation: $T_F = 110°C$, $(x_B)_F = 0.18$, $(x_T)_F = 0.01$.

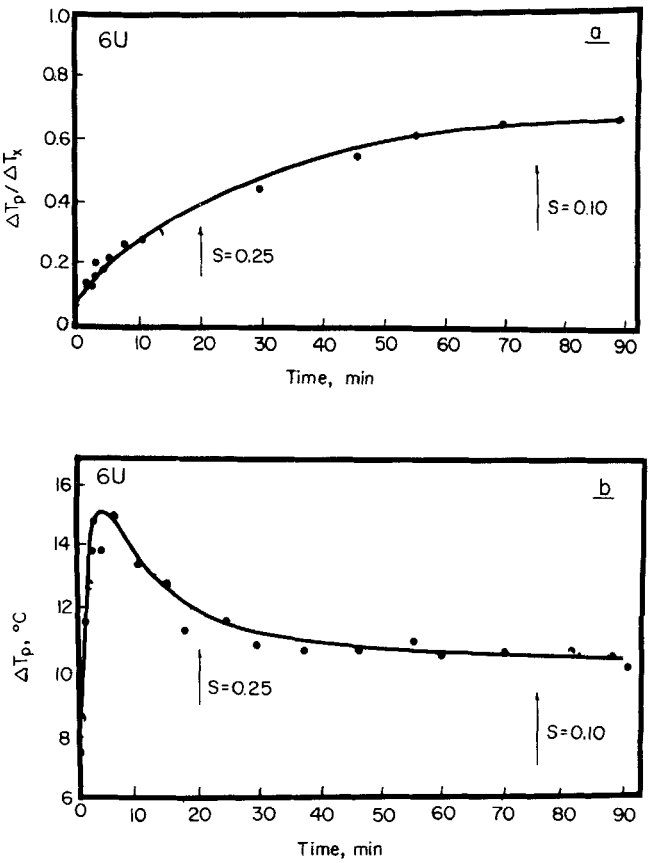

Fig. 6. History of the variation of intra-interphase gradients on catalyst poisoning. *a*. Increase of $\Delta T_p/\Delta T_x$ with time. *b*. Decrease of ΔT_p with time.

where a zone of complete deactivation apparently extends within the pellet for one quarter of the radius. The qualitative trends with decreasing activity are much as expected; the overall temperature gradient (bulk to center line) and the response time to final steady state both decrease with decreasing activity. Response time is not strongly affected by the poisoning, decreasing by about 30% in the examples here, although this increases to a factor of two to three in some runs at higher feed temperatures. We note also that there are measured maxima in the intraparticle profiles for most of the runs shown in Figures 3 and 4. The existence of such maxima had been indicated in prior simulation (Kehoe and Butt, 1972*a*) for fresh catalysts but had not been observed experimentally.

Some results of concentration-flow rate perturbation experiments on the series of catalysts of Figure 2 are illustrated in Figure 4. The trends in temperature gradients and response time are not clearly identifiable from the figure, per se, since differing magnitudes and directions of the perturbations are involved. However, the trends are indeed the same as for start-up transients, decreasing response time and temperature gradients with decreasing activity. Again, the influence of the outer deactivated zone for run 6-PP5 is clearly reflected in the temperature profiles.

Interphase-Intraphase Gradients

It is apparent from the results of both perturbation and start-up experiments that the ratio of intraphase to interphase temperature rise increases with the extent of deactivation, an unexpected result in light of the prior work of Koh and Hughes (1974). To explore this point further, one sample was further deactivated to a level $s = 0.10$. This extreme case of the response of a deactivated catalyst is shown in Figure 5; for a feed temperature of 110°C and benzene concentration of 18 mole %, the ratio of intra to interphase temperature rise exceeded two. The history of intra-interphase thermal gradients is shown in Figure 6*a* for run 6U; corresponding data on the activity vs. time for this sample were presented in Figure 1. It is seen that the ratio $(\Delta T_p/\Delta T_x)$ increases monotonically over the length of the run. This does not mean necessarily that ΔT_p increases with deactivation; in fact, it has a rather complicated history, as shown on Figure 6*b*, passing through a maximum $\Delta T_p = 15°C$ after about 5 min of poisoning ($s \approx 0.90$). A possible reason for maxima is that the surface temperature is immediately and strongly depressed on initiation of poisoning ($t = 0$ represents a steady state with fresh catalyst), while within the same time reference the center temperature remains constant at the initial value. The subsequent decrease in ΔT_p reflects the slowing down of the rate of decrease of surface temperature (that region is now completely deactivated) and the decrease in center temperature due to conduction. Such behavior is most strongly dependent on the reaction conditions (in these experiments it was observed at the lower feed temperatures and high benzene inlet concentrations) and the relative values of effective diffusivity and thermal conductivity of the pellet. Other experimental conditions led to a monotonic increase in ΔT_p on poisoning. Thus, in general, it was found that $(\Delta T_p/\Delta T_x)$ increased with deactivation in the range 0.1 to 0.4 to 0.5 from fresh to the most deactivated cases. These results on the relative magnitudes of inter to intraphase thermal gradients have been shown (Butt et al, 1977) to be in excellent agreement with theoretical predictions based on observables given by Carberry (1975). One is left with the

conclusion that the assignment of all thermal gradients to the boundary layer and all concentration gradients to the particle, even when based on good data for a fresh catalyst, may well break down as progressive deactivation occurs.

Hot Spot Migration

There have been several theoretical investigations of the migration of temperature maxima under unsteady conditions in single-pellet reaction (Hlavacek and Marek, 1971; Lee and Luss, 1970), and Hughes and Koh (1970) in experiments on ethylene hydrogenation on supported nickel observed movement of the transient profile maximum from the center to the surface.

Three different types of temperature maxima transients were observed in the present study, as illustrated in Figure 7. For experiments at low feed temperatures, the maximum moved quickly from the surface to the center of the pellet (run 1SI, $T_F = 50°C$), while for high feed temperatures, the hot spot remained close to the surface for most of the transient (run 2DEF2, $T_F = 188°C$). For intermediate feed temperatures, an excursion of the temperature maximum was observed in which the hot spot initially moved to the interior of the pellet, then moved back to the surface and remained there almost to the attainment of final steady state (runs 6P5, $T_F = 75°C$; 6U1, $T_F = 65°C$). These excursions were observed for both fresh and deactivated pellets and so cannot be attributed to any particular phenomenon associated with the poisoning. Physically, these excursions appear related to the rate of migration of the reaction zone and the concomitant depletion of reactant concentration and increase in temperature. Initially, the temperature at the surface is sufficiently low to permit penetration of the reactants into the interior of the pellet; after a period of time, the reaction within occurs at a sufficient rate to cause the temperature maximum to move away from the surface. For the proper conditions, however, the increase in surface temperature (occurring simultaneously) will be large enough in time to deplete reactant concentration in a region near the surface, thus forcing the temperature maximum back toward the surface. In this picture, then, the excursion of the hot spot appears due to an unsteady transition from intraparticle kinetic control to external mass transfer control. If external mass transfer is sufficiently rapid compared to the rate of reaction, a sufficient supply of reactant at the external surface is assured to permit the reaction zone to penetrate within the particle, and the hot spot would move continuously toward the center. The reverse situation obviously would tend to localize the maximum near the surface during the transient. Intermediate between these extreme cases, motion of the hot spot in both directions is possible.

This explanation is qualitatively supported by the magnitude of the Damköhler numbers for the runs illustrated in Figure 7. This quantity, defined as the ratio of the square of the Thiele modulus (at initial surface temperature) to the mass Biot number, expresses the relative magnitude of reaction kinetic to mass transport factors. It is seen that the values of N_{Da} characterizing the runs exhibiting temperature maximum excursions are, in fact, intermediate to the values determined for the two extreme cases.

Macroscopic Mechanism of Poisoning

When the rate of adsorption of poison on the catalytic sites is slow with respect to intraparticle diffusion, deactivation will be uniform throughout the pellet. On the other hand, if adsorption is rapid, the activity will be

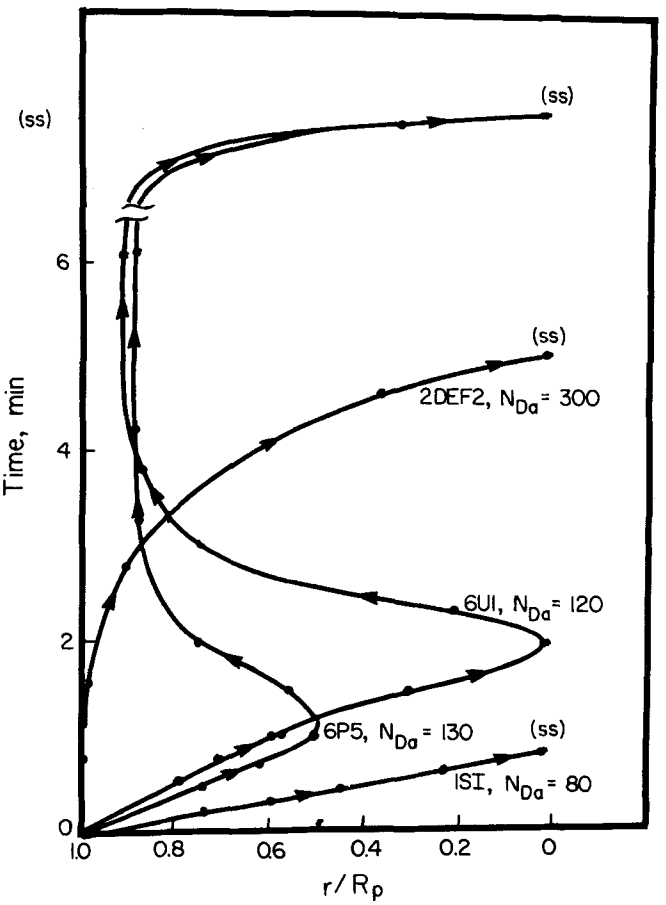

Fig. 7. Variations in hot spot migration patterns in start-up experiments.

nonuniform, and in the limit one would observe a zone of completely deactivated catalyst formed around the exterior, which moves toward the center as time progresses. This situation goes by various names such as pore mouth (Wheeler, 1955), shell progressive (Weisz and Goodwin, 1963), and core shrinking (Wang and Wen, 1972). We have already alluded to the fact that a number of the transient temperature profiles suggest strongly that such a shell progressive mechanism was prevalent under the present experimental conditions. Figure 8 shows a photograph of the cross section of

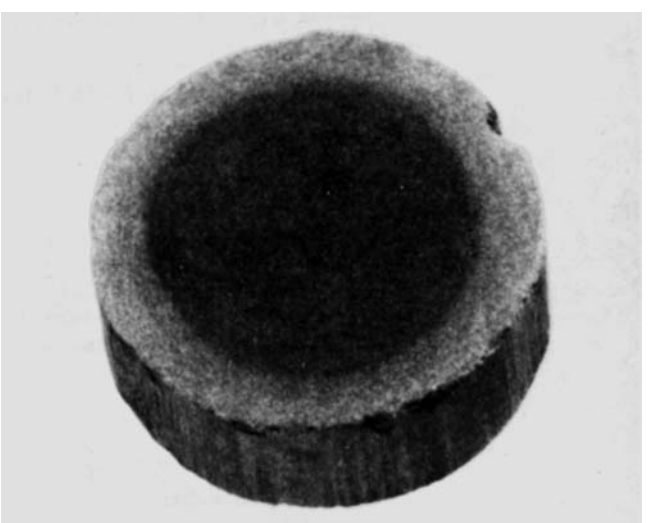

Fig. 8. Cross-section photograph of a deactivated catalyst particle: $T_F = 65°C$, $(x_B)_F = 0.16$, $(x_T)_F = 0.01$, $s = 0.16$ ($t = 90$ min).

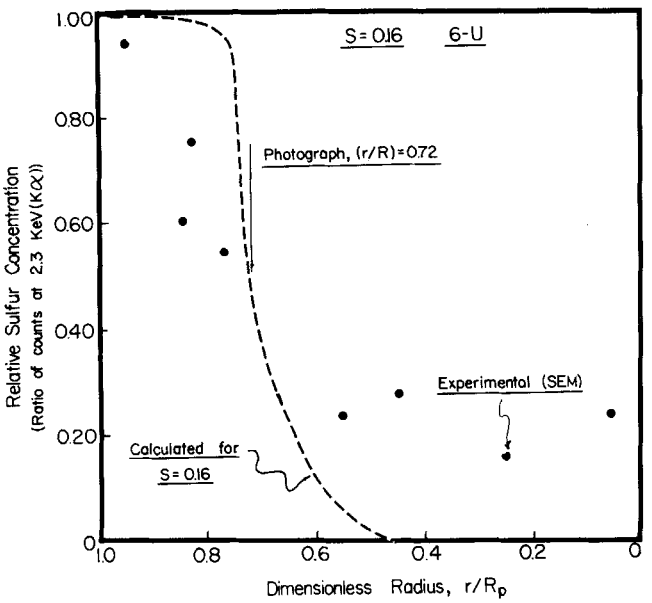

Fig. 9. Sulfur profiles in the particle of Figure 8.

the catalyst used in run 6-U after completion of the experiments ($s = 0.16$), after sectioning, polishing, and air calcining at 350°C for 2.5 hr. There is a distinct difference in coloration between the external shell and the core which is suggestive of some chemical alteration of the catalyst by contact with the poison. The matter was pursued further using a Kent Cambridge Stereoscan S4 scanning electron microscope with an EDAX microprobe. Sulfur was identified at 2.3 KEV (Kα), while other components were well separated at 7.46 KEV (nickel Kα) and 1.74 KEV (silicon Kα). A comparison between the results of the SEM probe and the approximate location of the shell boundary determined visually from the photograph is given in Figure 9 for the pellet of run 6U. The two measurements are in qualitative agreement as to position, although the SEM result indicates a less sharp division between shell and core than might be inferred from the photograph. Similar results were obtained for other catalysts used in the study.

SIMULATION

The preceding section has given an overview of the major trends observed experimentally and pointed out some of the principal changes in the transient behavior of the catalyst on deactivation. Now a major objective of this study has been to see how well one can do at a priori modeling of such behavior; such an approach requires the determination of the parameters required for mathematical description of the catalyst/reaction system by means independent of the transient response experiments insofar as possible. This necessitates separate experimentation (here for the kinetics of the main and poisoning reaction, catalyst thermal conductivity, density, and pore volume characteristics) or the use of reliable correlations (catalyst heat capacity, ratio of mass, and thermal Biot numbers). Additional factors (thermal Biot number, catalyst effective diffusivity) can be determined from the steady state experiments here and subsequently used in simulation of transients.

The experimental system is designed to conform to an infinitely long cylinder of catalyst, radially symmetric, with uniform composition and temperature in the surrounding reaction mixture. The appropriate conservation and rate equations are given in Table 3. In these equa-

Table 3. Mathematical Representation of the Reaction/Catalyst System

Conservation relations:

$$\frac{\partial C_B}{\partial t} = D_{eff}\,\nabla^2 C_B - s\,r_B(T, C_B)$$

$$\frac{\partial C_C}{\partial t} = D_{eff}\,\nabla^2 C_C + s\,r_B(T, C_B)$$

$$\frac{\partial C_T}{\partial t} = D_{eff}\,\nabla^2 C_T + \rho\,r_T(T, C_T)$$

$$\rho C_p \frac{\partial T}{\partial t} = \lambda_{eff}\,\nabla^2 T + (-\Delta H)\,s\,r_B(T, C_B)$$

$$\frac{ds}{dt} = r_d$$

Initial conditions:

$T = T_o(r)$

$s = 1$(fresh) or s(r) (deactivated)

$C_i = C_{io}(r);\ i = B, C, T$

Boundary conditions:

$(\partial C_i/\partial r)_o = (\partial T/\partial r)_o = (\partial s/\partial r)_o = 0$

$$D_{eff}\left(\frac{\partial C_i}{\partial r}\right)_{R_p} = k_g\,(C_{ib}(t) - C_i)$$

$$\lambda_{eff}\left(\frac{\partial T}{\partial t}\right)_{R_p} = h_T(T_b(t) - T)$$

Kinetic relationships:

$$r_B = \frac{a\exp(-F/RT)\,C_B}{1 + b\exp(H/RT)\,C_B};\quad r_d = -k_d^{\circ}\exp(-E_d/RT)\,C_T s$$

$$r_T = M_T\,r_d$$

TABLE 4

Parameters of mathematical model		Source
ϵ, D_{eff}, ρ, C_p, λ_{eff}	See Table 2	As indicated
$(-\Delta H)$	2.06×10^5 J/mole	
k_g	varies with experiment, see Table 5	This experiment
h_T	varies with experiment, see Table 5	This experiment
a	1.02×10^4 s^{-1}	Kehoe and Butt (1972)
b	1.70×10^{-4} m^3/mole	Kehoe and Butt (1972)
F	1.20×10^4 J/mole	Kehoe and Butt (1972)
H	3.68×10^4 J/mole	Kehoe and Butt (1972)
$k_d°$	4.09×10^{-1} m^3/mole-s (S.C.)	Weng et. al. (1975)
E_d	4.52×10^3 J/mole	Weng et. al. (1975)
M_T	$5.0 \pm 0.5 \times 10^{-4}$ mole/g	This experiment and Price and Butt (1977)

tions, it is assumed that hydrogen is present in essentially constant concentration, that the contribution of the poisoning to the energy balance is negligible in comparison to the heat of reaction, and that the poisoning kinetics can be represented as separable. By the latter it is meant that the reaction rate at any time is given by the product of the reaction rate on undeactivated catalyst times the activity variable s determined by the poisoning kinetics. The forms of the rate equations for hydrogenation and poisoning together with the associated kinetic and capacity parameters have been determined in separate experimentation and are discussed elsewhere by Kehoe and Butt (1972*b*) and Weng et al. (1975). The kinetic correlations given here have been developed for a rather narrow range of variables characteristic of the low benzene and high hydrogen concentrations employed in the experiments and are not intended to represent a general correlation. Values of the parameters involved in the simulation model are summarized in Tables 2, 4, and 5. In Table 5 are also presented values for a number of the dimensionless quantities which appear when the system of equations is cast into nondimensional form. Most of these are calculated directly from the parameters in Table 4; however, the heat and mass transfer coefficients and the corresponding Biot numbers were determined directly from experimentally observed reaction rate and film temperature gradient data by the overall temperature rise and rate of reaction using a modification of the analysis suggested by Lee and Luss (1969).

Numerical Solution

A Crank-Nicholson method combined with a shifted boundary technique (Von Rosenberg, 1969) was employed to solve the equations of Table 3. Full details of this procedure are given by Lee (1976). In addition to the solution for time-dependent temperature, concentration, and activity profiles, effectiveness factors were computed according to

$$\eta = \frac{D_{eff}(\partial C_B/\partial r)_{R_p}(2\pi R_p L)}{\dfrac{a \exp(-F/RT_{b_o})C_{Bb_o}}{1 + b \exp(H/RT_{b_o})C_{Bb_o}}(\pi R_p^2 L)} \quad (1)$$

TABLE 5. ADDITIONAL PARAMETERS AND DIMENSIONLESS QUANTITIES OF EXAMPLE SIMULATION RUNS

Run	x_{H_2}	x_B	T_b, °C	ΔT_x	ΔT_o	Rate (obs) ($\times 10$)	h_T	N_{Bi_h}	k_g ($\times 10^{-4}$)	N_{Bi_m}	N_{Le}	h (obs)	β	γ	γd	ξ	η (obs)
6DEF4	0.835	0.152	134.7	70.3	77.1	11.57	109.9	4.0	1.25	20.0	0.043	69.9	0.048	3.6	1.34	10.8	0.079
6P1	0.836	0.157	118.4	36.4	45.9	5.99	109.9	4.0	1.25	20.0	0.057	65.0	0.041	3.7	1.36	11.3	0.062
6PP3	0.838	0.159	118.2	16.1	26.5	2.65	109.9	4.0	1.25	20.0	0.057	64.9	0.043	3.7	1.39	11.3	0.026
6U1	0.831	0.157	96.6	85.1	92.6	14.02	109.9	4.0	1.25	20.0	0.043	58.2	0.065	3.9	1.48	11.9	0.304

Notes: $h_T = \text{J/m}^2\text{-s-°C}$
Rate $\equiv$ gmole/s-m^3
$k_g = \text{gmoles/m}^2\text{-s-}\Delta C$
$D_{eff} \equiv 3.0 \times 10^{-6}$ m^2/s for runs 6P1 and 6PP3
$D_{eff} \equiv 4.0 \times 10^{-6}$ m^2/s for runs 6DEF4 and 6U1

Dimensionless numbers:

$$N_{Bi_h} \equiv \frac{R_p h_T}{\lambda_{eff}} \qquad \beta \equiv \frac{C_{Bb} D_{eff}(-\Delta H)}{\lambda_{eff} T_B}$$

$$N_{Bi_m} \equiv \frac{R_p k_g}{D_{eff}} \qquad \gamma \equiv F/RT_b$$

$$\gamma d \equiv E_d/RT_b$$

$$N_{Le} \equiv \frac{\lambda_{eff}}{(\rho C_p)_{cat} D_{eff}} \qquad \xi \equiv H/RT_d$$

$$\eta \equiv \frac{\text{observed rate of reaction}}{\text{reaction rate at bulk conditions}}$$

$$h^2 \equiv \frac{R_p^2 a \exp(-F/RT_b)}{D_{eff}} \qquad T_b \equiv \text{bulk gas temperature at final steady state, °K}$$

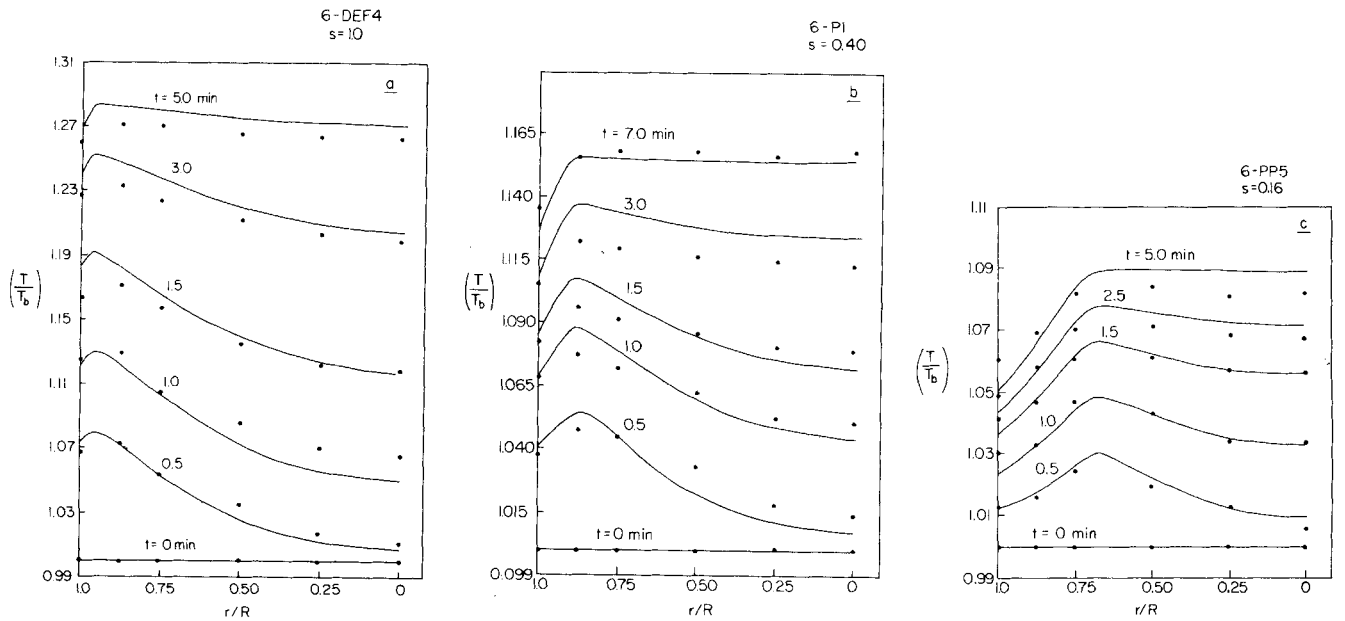

Fig. 10. Simulation of the effect of deactivation on start-up transients. *a.* $s = 1.0$; *b.* $s = 0.40$; *c.* $s = 0.16$.

and volume averaged activities by

$$\langle s \rangle = \frac{\int_o^{R_p} s(r,t)\,2\pi r L dr}{\pi R_p^2 L} \qquad (2)$$

The only tricky point in the numerical solution is that associated with the well-mixed behavior of the single-pellet reactor. In start-up and perturbation experiments, the bulk concentrations and temperature were time dependent, so that experimental values for $C_{ib}(t)$ and $T_b(t)$ were used in the boundary conditions in solution of the model for these cases. Values between the measured points were linearly interpolated. Concentration and temperature profiles obtained from the steady state solution were used as initial conditions for the perturbation simulations. Similarly, computed activity profiles were used as initial conditions in the simulation of the deactivated catalyst.

Results—Start-up

Typical results of the simulation for the two basic transient response experiments employed (start-up and perturbation) are shown in Figure 10 for a series of start-up runs on a progressively deactivated catalyst. Parameters employed in the simulation are given in Tables 2, 4, and 5. In general, the prediction of such transients by the model is good. The shape and temporal behavior of the thermal transients is well represented, and the simulation of the influence of deactivation on these factors is excellent. The wandering hot spots shown in Figure 7 are qualitatively modeled by the simulation, but no attempt was made to study this in detail because of the formidable requirements in computer time. Criticism may be made on some points, however: the simulation begins (fresh catalyst) by somewhat overpredicting surface temperatures and ends up ($s = 0.16$) by underpredicting them; indicated temperature maxima may be somewhat overpredicted, although in the case of run 6-PP we have no direct comparison with experimental measurements; and the final steady state computed for the most deactivated state is about 10% too high in terms of the reduced temperature variable (T/T_b). These factors point inferentially to some possible deficiencies in the representation of the deactivation mechanism or to difficulties associated with parametric sensitivity of the model.

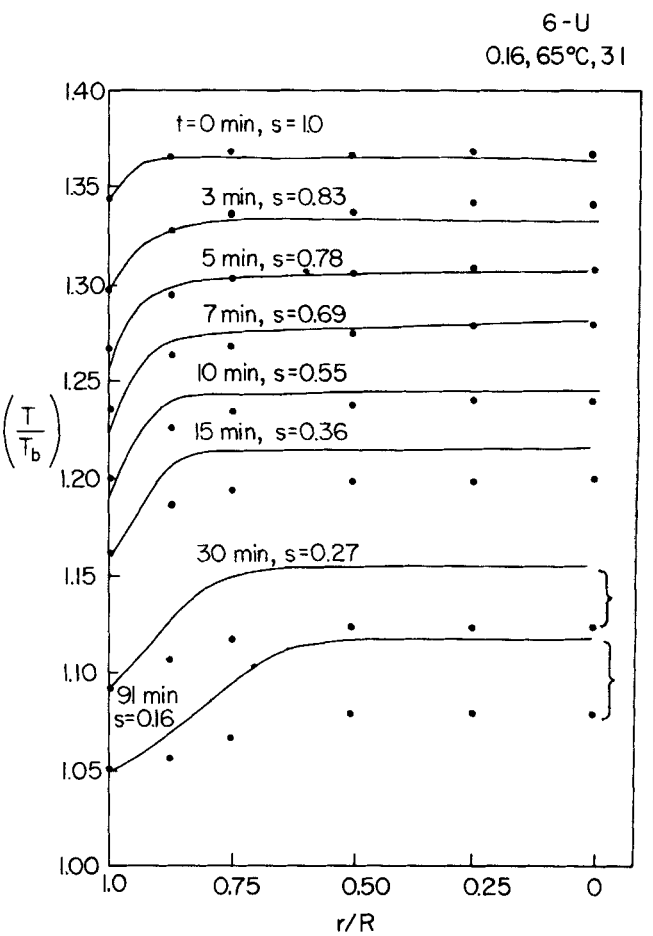

Fig. 11. Simulation of the history of intraphase gradients on progressive deactivation.

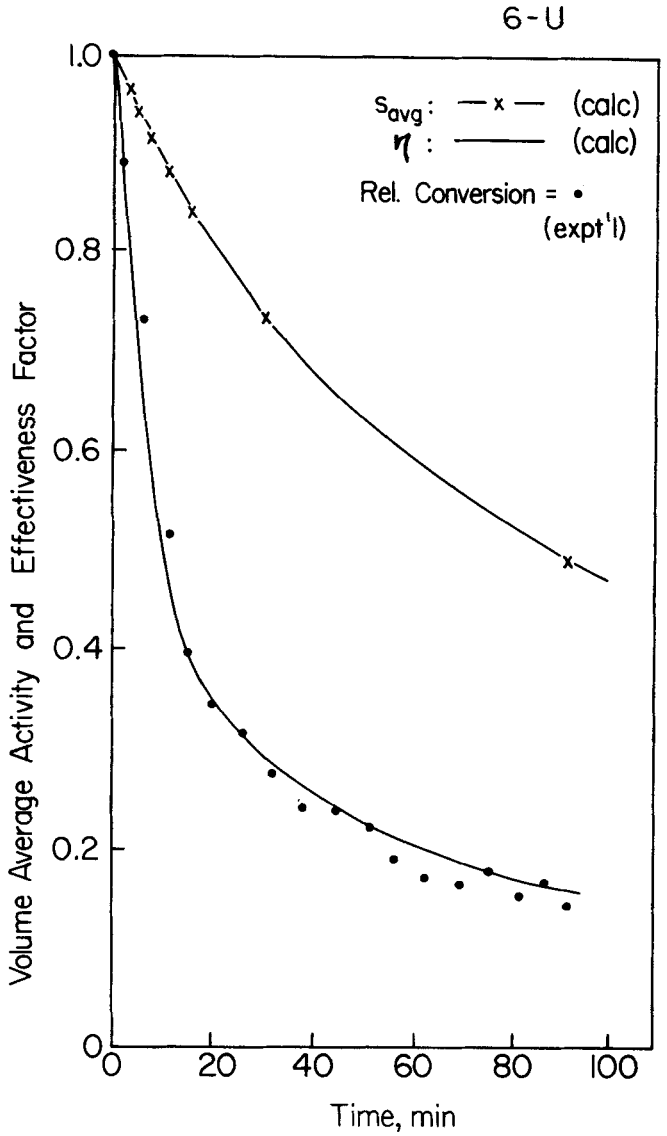

Fig. 12. Prediction of the history of overall activity on progressive deactivation.

Results—Progressive Deactivation

Simulation of the history of the intraparticle temperature profiles during deactivation is given in Figure 11. Again, it is seen that the simulation begins to run into some difficulty at the higher levels of poisoning. The results in this regard are in accord with Figure 10; in both cases, the simulation apparently attributes more activity to the catalyst than is the fact.

The calculated activity for run 6U at $s = 0.16$ is shown in comparison with the SEM results and photographic observation in Figure 9. Computation attributes a largely undeactivated zone in the catalyst extending out to $(r/R_p) \approx 0.7$, while the SEM data indicate a somewhat more broad distribution of sulfur. Now the SEM results can only be regarded as qualitative, since they are extracted from the baseline of a noisy signal;* hence we conclude that there is good agreement between computation and the two experiments here. In view of the steep gradients, a shell-progressive model could be considered adequate for simulation of the progressive deactivation of the particle. Simulation of transients in deactivated pellets by the shell model would be less satisfactory, since computed profiles are used as initial conditions in such calculations, and, while the activity profile of Figure 9 is sharp, it does not correspond exactly to the requirements of the shell model.

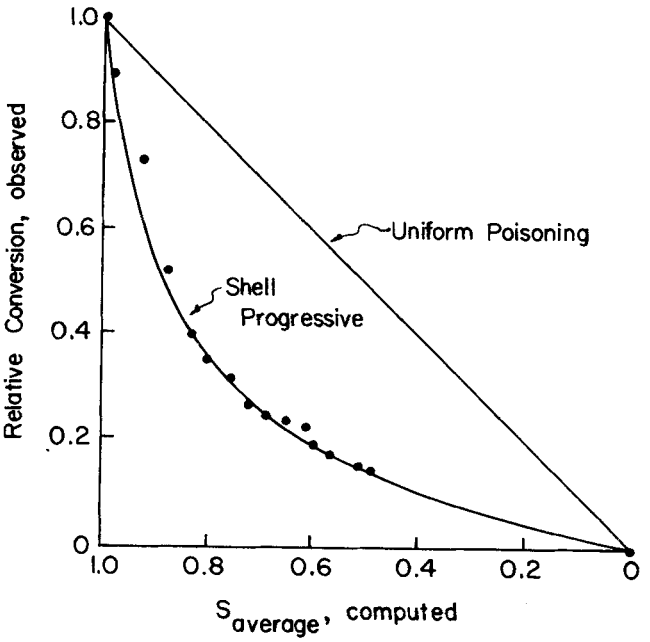

Fig. 13. Relationship between volume average activity and conversion.

Average Activity and Effectiveness Factor

The volume average activity obtained from computed profiles via Equation (2) for run 6U is compared with computed effectiveness factors and experimental data on relative conversion vs. time in Figure 12. The excellent agreement between predicted effectiveness and relative conversion reflects a compensation between actual and computed activity profiles. Referring again to Figure 9, one can see that the experimental and computed activity profiles do indeed indicate a type of compensation; the net area under each curve (hence, average activity) is about the same.

The large difference between the volume average activity and relative conversion is due to the diffusional retardation. In Figure 13, $<s>$ is plotted vs. the relative conversion as originally suggested by Wheeler (1955). The results are indicative of a strong, irreversible, poisoning mechanism and suggest that a shell-progressive mechanism is adequate for modeling overall activity-time behavior but less satisfactory in the more demanding task of simulation of transients or details of individual profiles.

On Parametric Values

The parameter set employed for the simulation here is generally adequate to the task, although arbitrary adjustment of D_{eff} between the limits of 3.0 and 4.0 $\times$ 10^{-6} m^2/s was employed to obtain the results illustrated. If, however, instead of using the modified Lee-Luss (1969) analysis to determine interphase transport coefficients, we determine them from measured temperature gradients, the volumetric rate of heat generation, and the relationship of Carberry (1966), a somewhat different set results (Butt et al., 1977). This parameter set can also be used to simulate the experimental results presented here, again using small variations in D_{eff} or h_T to force best fit. Now the differences in the two sets of parameters arise from variations in the influence of experimental error on individual values determined by different methods,

* We do not believe, for example, that sulfur has penetrated to the center of the particle.

so it seems unrealistic to think of the simulation problem in terms of a single, unique set of parameters. The combination of experimental uncertainty in parameter determination and parametric sensitivity of the model leads one to wonder whether attempts at a priori simulation in the detail demanded here are really ultimately feasible. At this point the question must remain unanswered.

ACKNOWLEDGMENT

This work was supported primarily by the National Science Foundation under GK 17200. Additional assistance was provided by the Mobil Foundation and Gould, Inc.

NOTATION

a = kinetic constant for benzene reaction rate, s^{-1}
b = adsorption constant for benzene reaction rate, m^3/mole
C_B, C_C, C_T = concentrations of benzene, cyclohexane and thiophene, mole/m^3
C_p = heat capacity of catalyst, J/kg-°C
C_{i_o} = initial concentration of component i, mole/m^3
C_b = bulk concentration, mole/m^3
D_{eff} = effective diffusivity, m^2/s
E_d = activation energy of poisoning rate, J/mole
F = temperature dependence of benzene kinetic constant, J/mole
H = temperature dependence of benzene adsorption constant, J/mole
$(-\Delta H)$ = heat of reaction, J/mole
h = Thiele modulus (Table 5)
h_T = heat transfer coefficient, J/m^2-s-°C
k_d = deactivation rate constant, m^3/mole-s
k_g = mass transfer coefficient, mole/m^2-s-ΔC
M_T = poison adsorption capacity, mole/g
N_{Bih}, N_{Bim} = Biot numbers for heat and mass transfer (Table 5)
N_{Da} = Damköhler number, h^2/N_{Bim}
N_{Le} = Lewis number (Table 5)
R = gas constant, J/mole-°C
R_p = particle radius, m
R_o = overall rate of reaction, mole/s-m^3
r = radial dimension, m
r_B, r_T = rate of reaction of benzene and thiophene, mole/s-m^3
r_d = rate of deactivation, s^{-1}
$s, \langle s \rangle$ = activity and average activity
T_F, T_b = feed and bulk temperature, °C
$\Delta T_p, \Delta T_x$ = intraparticle and interphase temperature differences, °C
ΔT_o = $\Delta T_p + \Delta T_x$
T_o = initial temperature, °C
t = time, s
$(X_B)_F, (X_T)_F$ = mole fraction of benzene and thiophene

Greek Letters

β = thermicity parameter (Table 5)
γ, γ_d = temperature sensitivity parameters (Table 5)
ϵ = catalyst porosity
η = effectiveness factor (Table 5)
λ_{eff} = effective thermal conductivity, J/m-s-°C
ξ = temperature parameter for adsorption (Table 5)
ρ = catalyst density, g/m^3
$(\rho C_p)_g$ = volumetric heat capacity of gas, J/m^3-°C

LITERATURE CITED

Aris, R., *The Mathematical Theory of Diffusion and Reaction in Permeable Catalysts*, The Clarendon Press, Oxford, England (1975).

Benham, C. B., and V. E. Denny, "Transient Diffusion of Heat, Mass Species and Momentum in Cylindrical Pellets during Catalytic Oxidation of CO," *Chem. Eng. Sci.*, **27**, 2163 (1972).

Butt, J. B., "Catalyst Deactivation," *Adv. Chem.*, **109**, 259 (1972).

———, D. M. Downing, and J. W. Lee, "Inter-Intraphase Temperature Gradients in Fresh and Deactivated Catalyst Particles," *Ind. Eng. Chem. Fundamentals*, **16**, No. 2, 270 (1977).

Carberry, J. J., "Yield in Chemical Reactor Engineering," *Ind. Eng. Chem.*, **58**, 40 (1966).

———, "On the Relative Importance of External-Internal Temperature Gradients in Heterogeneous Catalysis," *Ind. Eng. Chem. Fundamentals*, **14**, 129 (1975).

Hegedus, L. L., and E. E. Petersen, "Study of the Mechanism and Kinetics of Poisoning Phenomena in a Diffusion-Influenced Single Catalyst Pellet," *Chem. Eng. Sci.*, **28**, 69, 345 (1973).

Hlavacek, V., and M. Marek, "Effect of Heat and Mass Transfer inside Catalyst Particles on the Heterogeneous Catalytic Reaction," *Proceedings 4th European Symposium Chemical Reaction Engineering*, p. 107, Pergamon Press (1971).

Hughes, R., and H. P. Koh, "Intraparticle Temperature Measurements During Catalytic Reactions," *Chem. Eng. J.*, **1**, 186 (1970).

Irving, J. P., and J. B. Butt, "An Experimental Study of the Effect of Intraparticle Temperature Gradients on Catalytic Activity," *Chem. Eng. Sci.*, **22**, 1859 (1967).

Kehoe, J. P. G., and J. B. Butt, "Transient Response and Stability of a Diffusionally Limited Exothermic Catalytic Reaction," *Proceedings 2nd International Symposium Chemical Reaction Engineering*, p. B8-13, Elsevier, Amsterdam (1972*a*).

———, "Interactions of Inter- and Intraphase Gradients in a Diffusion Limited Catalytic Reaction," *AIChE J.*, **18**, 347 (1972*b*).

Koh, H. P., and R. Hughes, "Catalyst Temperature Profiles Under Poisoned Conditions," *ibid.*, **20**, 395 (1974).

Lee, J. C. M., and D. Luss, "Maximum Temperature Rise Inside Catalytic Pellets," *Ind. Eng. Chem. Fundamentals*, **8**, 596 (1969).

———, "The Effect of Lewis Number on the Stability of a Catalytic Reaction," *AIChE J.*, **16**, 620 (1970).

Lee, J. W., "Effects of Intraparticle Deactivation on Catalyst Performance," Ph.D. dissertation, Northwestern University, Evanston, Ill. (1976).

Lyubarskii, G. B., L. B. Andeera, and N. V. Kul'kova, "Study of Thiophene Poisoning of Nickel Catalysts," *Kin. Kat.*, **3**, 123 (1962).

Price, T. H., and J. B. Butt, "Catalyst Poisoning and Fixed Bed Reactor Dynamics, II. Adiabatic Reactors," *Chem. Eng. Sci.*, **32**, 393 (1977).

Trimm, D. L., J. Corrie, and R. D. Holton, "The Measurement and Prediction of Temperature Increase in Single Catalyst Pellets," *ibid.*, **29**, 2009 (1974).

Von Rosenberg, D. U., *Methods for the Numerical Solution of Partial Differential Equations*, American Elsevier, New York (1969).

Wang, S. C., and C. Y. Wen, "Experimental Evaluation of Nonisothermal Solid-Gas Reaction Model," *AIChE J.* **18**, 1231 (1972).

Weisz, P. B., and R. B. Goodwin, "Combustion of Carbonaceous Deposits with Porous Catalyst Particles I. Diffusion-Controlled Kinetics," *J. Catal.*, **2**, 397 (1963).

Weng, H. S., G. Eigenberger, and J. B. Butt, "Catalyst Poisoning and Fixed Bed Reactor Dynamics," *Chem. Eng. Sci.*, **30**, 1341 (1975).

Wheeler, A., *Catalysis*, P. H. Emmett, ed., Vol. 2, Chapt. 2, Reinhold, New York (1955).

Wolf, E., and E. E. Petersen, "Theoretical Analysis of Poisoning in a Single-Pellet Diffusion Reactor for Main Reactions Not of First Order," *Chem. Eng. Sci.*, **29**, 1500 (1974).

Manuscript received May 16, 1977; revision received November 8, and accepted December 7, 1977.